

Study on Effects of Wood Fiber Content on Physical, Mechanical, and Acoustical Properties of Wood-fiber-filled Gypsum Composites

Hamed Ramezani^{a*}, Sina Shahdab^b, Ali Nouri^c

^aYoung Researchers Club, Islamic Azad University, Shahrerey Branch, Tehran, Iran

^bFaculty of Agriculture, Islamic Azad University, Chalus Branch, Chalus, Iran

^cDepartment of Aerospace Engineering, Satari University, Tehran, Iran

Received: June 1, 2011; Revised: January 20, 2012

The Acoustical model of wood-fiber-filled gypsum composites panel is presented. The transmission loss coefficients of the composite structures were calculated by an approximated approach. However, the physical and mechanical properties of board specimens including; water absorption, thickness swelling, bending modulus of elasticity, bending modulus of rupture, internal bond, and compression parallel to the surface obtained experimentally. Finally, the effects of wood fibers to gypsum mixing ratios on physical, mechanical and acoustical properties of composite flat structures were investigated and data analysis was done by use of statistical methods.

Keywords: *mechanical and physical properties, acoustic, transmission loss, wood-fiber-filled gypsum composite, Analysis of Variance (ANOVA)*

1. Introduction

The interaction between an acoustic wave and a wood-fiber-filled gypsum board composites panel is an important subject that arises from practical application. These panels consist of short wood fibers, gypsum, water and additive materials. The fibers have important role in the composite properties; therefore there are comprehensive investigations of different aspects of fibers affects on this category of structures, i.e. fiber characteristics¹, different behaviors of synthetic fibers² and cellulosic fibers³ contrary to natural fibers⁴.

Effect of the fiber content as another important parameter in short-fiber reinforced composites studies should be considered. In fact, just as the fibers cause increasing of stiffness of composite structures, so in the composite material provide stress concentrations, therefore providing sites for crack initiation. Crack initiation and propagation occur at the fiber/matrix interface as a result of the poor interface between materials⁵. The interface is weak when the fiber proportion in the composite material is high. It is typical to assume that the composite boards are three-dimensional isotropic when the fibres length are much less than the thickness of the part⁶⁻⁸. Modeling is based on the concept of averaging the elastic constants over all possible orientation of fibers which is done by integration. These models with different degree of approximation are inadequate to predict the mechanical and physical properties of short fiber-reinforced composites; therefore the experimental tests were done by authors.

Wood-fiber-filled gypsum composites are used in the construction of walls in offices, educational establishments, or laboratories, therefore acoustic performance as well

as mechanical properties in designing is very important. Therefore the prediction of transmission loss through composite specimens is very important. Acoustic design involves elastic wave propagation in materials and interaction of sound waves with the structures. Many analytical methods attempt to describe the vibro-acoustic behavior of structures explicitly and resolve the associated variations in response over space and time. Koval⁹ considered the aircraft fuselage as an infinite cylindrical shell and investigated several areas relevant to the interior noise problem. Blaise et al.¹⁰ extended Koval's studies to the case of a plane acoustic wave with two independent angles of incidence in order to calculate the diffuse field transmission coefficient of an orthotropic shell. Roussos et al.¹¹ gave a report made in the NASA Langley Research Center about the theoretical and experimental study of noise transmission through composite plates. Analytical and experimental studies are conducted by Lee and Kim sound transmission through the infinitely long circular cylindrical shell¹². Daneshjou et al.^{13,14} obtained an exact solution to calculation of the transmission loss of orthotropic and laminated composite cylindrical shells by considering all three displacements of the shell. Harris¹⁵ studied acoustic emission through flat panels. Lin et al.¹⁶ investigated Sound transmission loss across orthotropic composite laminate.

The literature clearly shows that, there is no analytical investigation on acoustic transmission of wood-fiber-filled gypsum composites board, in spite of the fact that the quantity of transmission loss of this plate is important to their applications. In this study flat wood-fiber-filled gypsum board composite structures with different fibers proportions were made and then Bending Modulus of Elasticity

*e-mail: h_ramezani@mecheng.iust.ac.ir

(MOE), Bending Modulus of Rupture (MOR), Internal Bond (IB) and Compression parallel to the surface (C_{\parallel}) for each specimen were measured. In addition, two physical properties that are Water Absorption ($WA_{2,24}$) and Thickness Swelling ($TS_{2,24}$) after 2 and 24 hours submersion measured; finally the Transmission Loss (TL) through composite board specimens is calculated by an analytical method.

2. Specimen Preparation

Wood fibers were derived from manufacture line of a local MDF producer, ranging from approximately 2 to 4 mm long. After the wood fibers were dried, they were screened by 8-mesh screen and then blended with Beta-hemihy-drate gypsum powder (Table 1) at 10, 15, 20, 25, or 30% by dry weight. Paste was then added to composite materials at a level of 0.5% based on dry gypsum weight to increase the time of setting. The stirring operation was continued uniformly using a blender (2000 rpm) for about 5 minutes. Meanwhile the water was pouring gradually into the mixture. Water and gypsum for each mixture had a weight ratio of 40:100. The stirring duration, which is, the time of elapsing between beginning of the stirring operation and pouring the mixture into a mold, limited to 10 minutes. After that the mixture was poured in the mold which was cubic (40 by 40 by 1 cm). Then it was pressed at a rate of 20 kg.cm⁻² using a cold pressure for 25 minutes. Then the specimens (Figure 1) were placed in ambient air about 30 minutes, and then cut into standard sizes. Moisture content at this moment was 16 to 20, thus specimens were placed in the drying oven at about 75 °C. Drying operation was continued until the humidity reached about 1 to 2 %.

3. Experiment Procedure

The mechanical and physical properties were determined in accordance with ASTM standard D 1037-99^[17,18]. The specimens were loaded in bending test until failure occurs at a rate of 5 mm/min. The experiments were done by using an INSTRON Testing Machine. This operation was repeated five times for each specimen.

4. Transmission Loss of Board Specimens

The board can be modeled as a one-dimensional beam vibro-acoustic problem therefore; the beam motion represents the motion of the board. Figure 2 showed a schematic of a unit-width beam subjected to a plane wave with an incidence angle γ . In this model, it is typical to idealize the system as an infinitely long beam that divides two semi-infinite acoustic media. The acoustic media in the incident and transmitted sides of the beam are defined by the density and the speed of sound: $\{s_1, c_1\}$ and $\{s_3, c_3\}$ respectively.

In the fluid (acoustic) media, the wave equation becomes¹² (Equations 1 and 2):

$$c_1 \nabla^2 (p^I + p_1^R) + \frac{\partial^2 (p^I + p_1^R)}{\partial t^2} = 0 \tag{1}$$

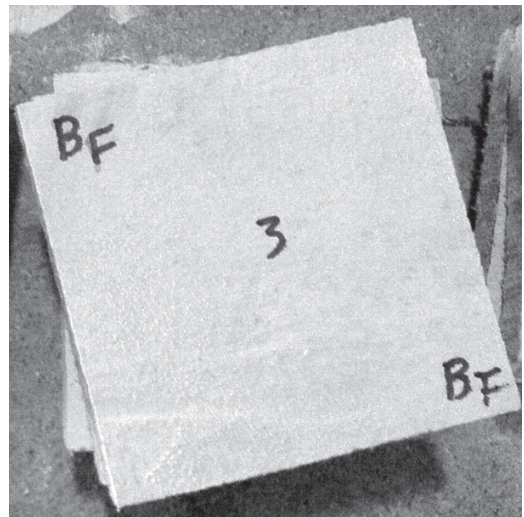


Figure 1. A wood fiber/gypsum board composites sample.

Table 1. Chemical and physical characteristics of the Beta-hemihy-drate gypsum.

Properties		Standards		Natural gypsum
		NBR* 13207	NFB** 12300/63	
Chemical analysis (%)	Water of crystallization	4.2 to 6.2	-	7.75
	CaO	>38	-	38.73
	SO ₃	>53	>45	52.13
	Al ₂ O ₃ + Fe ₂ O ₃	-	-	0.42
	SiO ₂ + RI	-	-	0.67
	Calculated chemical percentage (%)	CaSO ₄ .1/2 H ₂ O	-	-
PH	CaSO ₄	-	-	-
	CaSO ₄ .2 H ₂ O	-	-	3.3
		-	-	7.94
Physical properties	Specific mass (g.cm ⁻³)	>1.10 (Thick foundry gypsum)		2.40
	Thickness factor	<1.10 (Thin foundry gypsum)		0.71
	Unit mass (kg.m ⁻³)	>700.00		652.00

*British standard. **French standard.

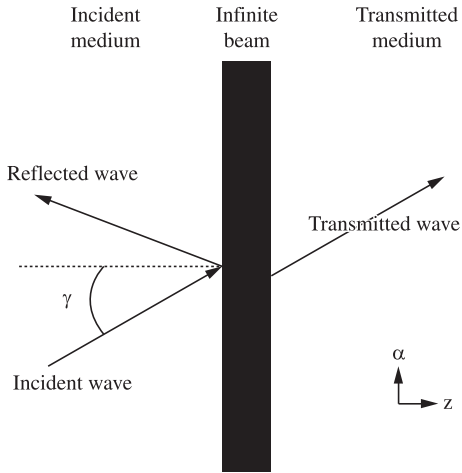


Figure 2. Schematic of an infinite beam model.

$$c_3 \nabla^2 (p_3^T) + \frac{\partial^2 (p_3^T)}{\partial t^2} = 0 \tag{2}$$

where ∇^2 is the Laplacian operator in the rectangular coordinate and p^I , p_1^R , and p_3^T are the acoustic pressures of the incident, reflected, and transmitted waves, which given as (Equations 3, 4 and 5);

$$p^I = p_0 e^{j(\omega t - \xi_{1\alpha} \alpha - \xi_{1z} z)} \tag{3}$$

$$p_1^R = p_{1n}^R e^{j(\omega t - \xi_{1\alpha} \alpha + \xi_{1z} z)} \tag{4}$$

$$p_3^T = p_{3n}^T e^{j(\omega t - \xi_{3\alpha} \alpha - \xi_{3z} z)} \tag{5}$$

where p_0 , p_{1n}^R , and p_{3n}^T are the amplitudes of the waves, $n = 0, 1, 2, 3, \dots$ indicates the mode number, $j = \sqrt{-1}$, and ω is the angular frequency. In Equations 3 and 4 ξ_1 , wave number in the incident medium, is defined as $\xi_{1\alpha} = \omega/c_1$, $\xi_{1\alpha} = \xi_1 \sin \gamma$, $\xi_{1z} = \xi_1 \cos \gamma$ and in Equation 5 ξ_3 , wave number in the transmitted medium, is defined as $\xi_3 = \omega/c_3$,

$$\xi_{3\alpha} = \xi_3 \alpha, \quad \xi_{3z} = \sqrt{\xi_3^2 - \xi_{3\alpha}^2}$$

Equation of motion of the beam can be written as¹² (Equation 6);

$$-(1/12)Eh^3 \frac{\partial^4 w^0}{\partial \alpha^4} = \rho h \frac{\partial^2 w^0}{\partial t^2} + p_z \tag{6}$$

where E , ρ , and h are the Young modulus, density and the thickness of the beam, respectively. In Equation 6 w^0 , the displacement of the beam's midsurface in the α direction, and p_z , the body force component normal to the beam midsurface is given by (Equations 7 and 8);

$$w^0 = w_n^0 e^{j(\omega t - \xi_{1\alpha} \alpha)} \tag{7}$$

$$p_z = p_3^T - (p^I + p_1^R) \tag{8}$$

The boundary conditions at the two interfaces between the beam and fluids can be represented as¹² (Equations 9 and 10):

$$\frac{\partial^2 (p^I + p_1^R)}{\partial z} = -s_1 \frac{\partial^2 w^0}{\partial t^2} @ z = 0 \tag{9}$$

$$\frac{\partial^2 p_3^T}{\partial z} = -s_3 \frac{\partial^2 w^0}{\partial t^2} @ z = h \tag{10}$$

By substitution of the Equations 3, 4, 5, and 7 into Equations 6, 9, and 10 yields 3 equations. Therefore the three unknown amplitudes p_{1n}^R , p_{3n}^T , and w_n^0 can be obtained in terms of p_0 by solving these three equations for each mode n .

The transmission coefficient $\tau(\gamma)$ is the ratio of the amplitudes of the incident and transmitted waves. $\tau(\gamma)$ is a function of the incidence angle γ defined by¹² (Equation 11):

$$\tau(\gamma) = \sum_{n=0}^{\infty} \frac{\text{Re} \left\{ p_{3n}^T \times (j\omega w_n^0)^* \right\} s_1 c_1}{2 \cos(\gamma) p_0^2} \tag{11}$$

$\text{Re} \{ \}$ and the superscript $*$ represents the real part and the complex conjugate of the argument. To consider the random incidences, $\tau(\gamma)$ can be averaged according to the Paris formula¹⁹ (Equation 12):

$$\bar{\tau} = 2 \int_0^{\gamma_m} \tau(\gamma) \sin \gamma \cos \gamma d\gamma \tag{12}$$

where γ_m is the maximum incident angle. Integration of Equation 12 is conducted numerically by Simpson's rule. Finally, the average value of TL is obtained as (Equation 13):

$$TL_{avg} = 10 \log \frac{1}{\bar{\tau}} \tag{13}$$

In the following, the averaged TL of the structure is calculated in terms of the 1/3 octave band for random incidences.

5. Convergence Algorithm

Equations 4, 5, and 7 are obtained in series form. Therefore, enough numbers of modes should be included in the analysis to make the solution be converged. When the TL calculated at two successive calculations are within a pre-set error bound, the solution is considered to have converged. An iterative algorithm for the calculation of TL at each frequency is;

```

REPEAT
    TLn = 10 log 1/τ̄
    Set n = n + 1
UNTIL |TLn+1 - TLn| < 1e-6
    
```

6. Results and Discussion

Fiber and gypsum for each board specimen had a weight ratio of 10:90, 15:85, 20:80, 25:75, or 30:70 hereafter called X1, X2, X3, X4, and X5, respectively. Also gypsum board specimen called X0.

The board specimens had significant difference in the WA, TS, MOR, MOE, IB and $C_{||}$ values. Table 2 showed the physical and measured mechanical properties of the specimens X0 to X5 groupings, which is a significant difference ($p < 0.01$) between groups determined individually for tests by Duncan’s multiple comparison tests.

During the hydration reaction of gypsum, the fibers are bonded to hydrates. However, by decreasing of fiber proportion and increasing of dehydrate crystals in wood-gypsum material the bonding process proceeds better which reduced thickness swelling of the boards. Therefore, as results showed dimensional stability of the specimens X0, X1, X2, and X3 and only the specimens X0 and X1 are better than the others as a result of $TS_{2,24}$ tests, respectively. Also, the specimen X0 showed the highest water resistance after WA tests, while the highest WA values were found for the specimen X5. Tends to enhance the availability of the hydroxyl groups (absorption sites), by increasing of the fiber proportion in composite material could be reason for this finding.

The results also presented the specimens had significant difference in strength tests. As Table 2 shows the specimens X1 and X5 had the greatest and lowest MOR, MOE, IB and $C_{||}$ values, respectively. In fact, the wood fibers in the gypsum matrix provided stress concentrations, therefore providing sites for crack initiation. Crack initiation and propagation occurred at the wood fiber/gypsum interface as a result of the poor interface between materials⁵. Thus, the more content of the wood fibers, the larger the stress concentration along the weak interface of the wood fiber and gypsum, and the lower strength is why X1 specimen has better structural performance along the other ones. Furthermore, the reasons for this finding can be attributed to many other facts such as differential shrinkage between the fibers and gypsum, which produces interface shear stresses leading to interface de-bonding. In other word, the fundamental parameter in designing of composite material is that there must be exists the optimization of the volume fraction of fibers to matrix.

To validate the one-dimensional model of sound transmission through structure a comparison between TL values of the numerical model and experimental results (Harris’ study¹⁵) is presented. In Harris’ work, the size of the experimental specimen (121.92 by 243.84 cm) can be considered very large in comparison to the limited thickness (0.8 mm) of the plate. As showed in Figure 3, the numerical results have a good agreement with the experimental results except at very low frequency region, where the finite size and boundary conditions of the structure become important. It is due to the fact that the numerical model is based on an infinite beam, while the experimental study is limited to a finite specimen.

Parametric numerical studies of TLs are conducted for infinite beams specified as follows, in 1/3 octave band frequency. Material density and thickness of the beams are $\rho = 1000 \text{ kg.m}^{-3}$ and $h = 0.01 \text{ m}$, respectively. Average values of E , longitudinal modulus of elasticity, determined by bending test¹⁸ are given in Table 3 for specimens. Density and sound of speed in incident and transmitted media are 1.2 kg.m^{-3} and 343 m/s , respectively.

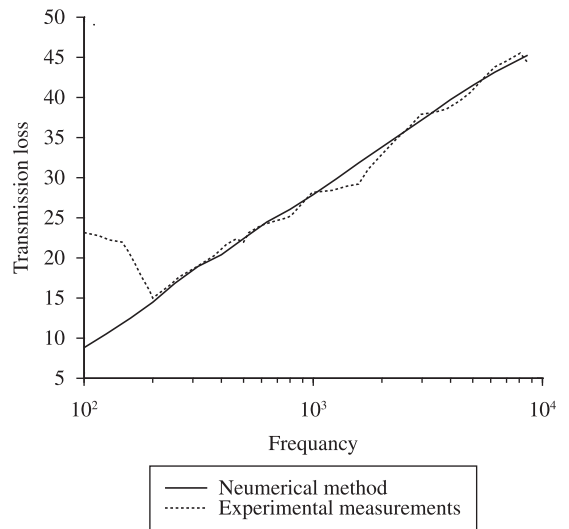


Figure 3. Comparison between TL curves of the approximate values and the experimental measurements (taken from Harris¹⁵). The physical and geometrical parameters are: Young’s modulus; $E = 206 \text{ GPa}$, Density; $\rho = 78000 \text{ kg.m}^{-3}$, and beam thickness; $h = 0.8 \text{ mm}$.

Table 2. Average values of physical and mechanical tests of board specimens made with difference mixture ratio.

Sample	Mechanical properties				Physical properties			
	MOE (MPa)	MOR (MPa)	IB (MPa)	$C_{ }$ (MPa)	TS (%)		WA (%)	
					2*	24	2	24
X0	2.7823e3 B**	1.8920 B	0.6200 B, C	4.4000 B	0.5833 A	1.8150 A	17.2337 A	19.5200 A
X1	3.9297e3 A	3.5167 A	0.8867 A	8.7833 A	0.6670 A	2.4498 A, B	24.6490 B	27.4223 B
X2	3.1049e3 B	3.0333 A	0.7483 A, B	4.9333 B	0.7608 A	2.6535 B	32.4273 C	35.9602 C
X3	1.0776e3 C	1.3000 C	0.5783 B, C	2.5667 C	0.7867 A	3.0170 B	45.1103 D	47.0967 D
X4	0.7443e3 C	0.7667 D	0.4833 C	1.1667 D	1.1402 B	4.2038 C	55.1777 E	59.6405 E
X5	0.2389e3 D	0.5000 D	0.2917 D	0.8667 D	1.8908 C	4.4252 C	70.8540 F	75.1093 F

*Hours for TS and WA tests. **Homogenous groups; same capital letters in each column indicate that there is no statistical difference between the samples.

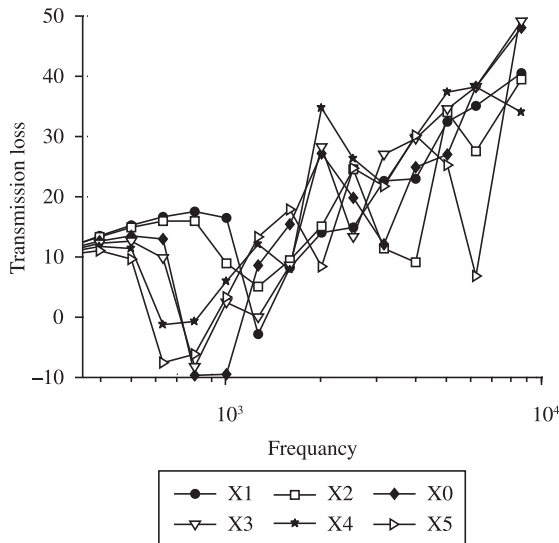


Figure 4. Comparison between TL curves for the X0 to X5 specimens.

Figure 4 compared the TL curves of specimens X0 to X5. The results represented a desirable level of TL in the frequency range lower than 1000 Hz for board specimen X1, which had the highest strength value. As results showed the mixture ratio of composite material is effective on TL curve, especially on Stiffness-controlled region (Frequencies lower than resonant freq.). However, no clear preference depicted in Mass-controlled region (Frequencies higher than resonant freq.), because all samples had the same mass and dimensions. The effect of thickness of the beam on TL is showed in Figure 5. As showed in this figure, changing the thickness of the beam had a broadband effect on TL over the entire range of the frequency.

7. Conclusion Remarks

This study investigated to represent the effect of mixing ratio of wool fiber to gypsum on the physical,

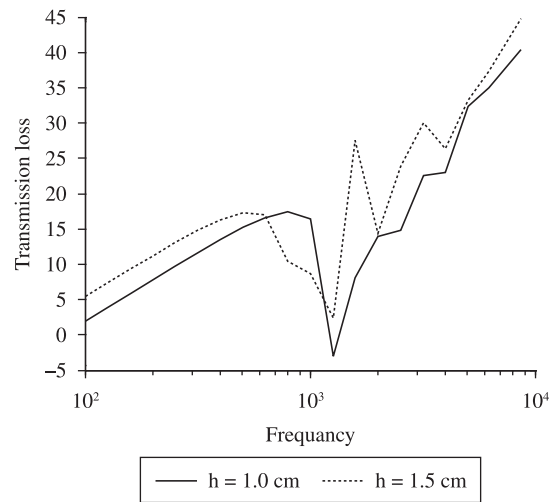


Figure 5. Comparison between TL curves for the X1 specimen with respect to beam thickness.

mechanical, and acoustical properties of board composites. Fiber and gypsum for each board composite had a weight ratio of 10:90, 15:85, 20:80, 25:75, or 30:70. The explicit conclusions of this work, regard to six types of samples, are:

- 1) Composites made with less fiber content were found to have better physical properties;
- 2) Decreased fiber content significantly increased strength of structures;
- 3) Decreasing of fiber proportion in composite material of board specimens tends to enhance the TL curve at low frequencies;
- 4) By changing the fiber proportion, there was no clear preference in TL curves at mid frequencies: and
- 5) Changing the thickness of the beam had a broadband effect on TL over the entire range of the frequency.

References

1. Bouafif H, Koubaa A, Perré P and Cloutier A. Effects of fiber characteristics on the physical and mechanical properties of wood plastic composites. *Composites: Part A*. 2009; 40:1975-1981. <http://dx.doi.org/10.1016/j.compositesa.2009.06.003>
2. McHenry E and Stachurski ZH. Composite materials based on wood and nylon fibre. *Composites: Part A*. 2003; 34:171-181. [http://dx.doi.org/10.1016/S1359-835X\(02\)00211-7](http://dx.doi.org/10.1016/S1359-835X(02)00211-7)
3. Dalmay P, Smith A, Chotard T, Sahay-Turner P, Gloaguen V and Krausz P. Properties of cellulosic fibre reinforced plaster: influence of hemp or flax fibres on the properties of set gypsum. *Journal of Materials Science*. 2010; 45(3):793-803. <http://dx.doi.org/10.1007/s10853-009-4002-x>
4. Herrera-Franco PJ and Valadez-Gonzalez A. A study of the mechanical properties of short natural-fiber reinforced composites. *Composites: Part B*. 2005; 36:597-608. <http://dx.doi.org/10.1016/j.compositesb.2005.04.001>
5. Carvalho MA, Calil Júnior C, Savastano Junior H, Tubino R and Carvalho MT. Microstructure and mechanical properties of gypsum composites reinforced with recycled cellulose pulp. *Materials Research*. 2008; 11(4).
6. Nielsen LE and Chen PE. Young's Modulus of Composites Filled with Randomly Oriented Fibers. *Journal of Materials*. 1968; 3(2):352-358.
7. Halpin JC and Pagano NJ. The Laminate Approximation for Randomly Oriented Fibrous Composites. *Journal of Composite Materials*. 1969; 3:720-724
8. Chen PE. Strength Properties of Discontinuous Fiber Composites. *Polymer Engineering and Science*. 1971; 11(1):51-55. <http://dx.doi.org/10.1002/pen.760110109>
9. Koval LR. On sound transmission into an orthotropic shell. *Journal of Sound and Vibration*. 1979; 63:51-59. [http://dx.doi.org/10.1016/0022-460X\(79\)90376-6](http://dx.doi.org/10.1016/0022-460X(79)90376-6)

10. Blaise A, Lesuer C, Gotteland M and Barbe M. On sound transmission into an orthotropic infinite shell: Comparison with Koval's results and understanding of phenomena. *Journal of Sound and Vibration*. 1991; 50:233-243. [http://dx.doi.org/10.1016/0022-460X\(91\)90618-T](http://dx.doi.org/10.1016/0022-460X(91)90618-T)
11. Roussos LA, Powell CR, Grosveld FW and Koval LR. Noise transmission characteristics of advanced composite structure materials. *Journal of Aircraft*. 1984, 21(7), 528-535. <http://dx.doi.org/10.2514/3.45003>
12. Lee JH and Kim J. Study on sound transmission characteristics of a cylindrical shell using analytical and experimental models. *Applied Acoustics*. 2003, 64, 611-632. [http://dx.doi.org/10.1016/S0003-682X\(02\)00138-X](http://dx.doi.org/10.1016/S0003-682X(02)00138-X)
13. Daneshjou K, Nouri A and Talebitooti R. Sound Transmission Through Laminated Composite Cylindrical Shells Using Analytical Model. *Archive of Applied Mechanics*. 2007; 77:363-379. <http://dx.doi.org/10.1007/s00419-006-0096-7>
14. Daneshjou K, Nouri A and Talebitooti R. Analytical model of sound transmission through orthotropic cylindrical shells with subsonic external flow. *Aerospace Science and Technology*. 2009; 13:18-26. <http://dx.doi.org/10.1016/j.ast.2008.02.005>
15. Harris DA. *Noise Control manual*. New York: Van Nostrand Reinhold; 1991.
16. Lin HJ, Wang CN and Kuo YM. Sound transmission loss across orthotropic composite laminate. *Applied Acoustics*. 2007; 68(10):1177-91. <http://dx.doi.org/10.1016/j.apacoust.2006.06.007>
17. British Standard Institution. *BS 1191: Part 1. Specification for gypsum building plasters*. London: BSI; 1973.
18. American Society for Testing and Materials – ASTM. *ASTM D 1037-99: Test Methods for Evaluating Properties of Wood-Base Fiber and Particle Panel Materials Wood*. Annual Book of ASTM Standards; 2009.
19. Pierce AD. *Acoustics*. New York: McGraw-Hill; 1981.